

Characterization of solid-state forms of celecoxib

Garima Chawla^a, Piyush Gupta^a, R. Thilagavathi^b,
Asit K. Chakraborti^b, Arvind K. Bansal^{a,*}

^a Department of Pharmaceutical Technology (Formulations), National Institute of Pharmaceutical Education and Research (NIPER), S.A.S. Nagar, Punjab 160 062, India

^b Department of Medicinal Chemistry, National Institute of Pharmaceutical Education and Research (NIPER), S.A.S. Nagar, Punjab 160 062, India

Received 17 April 2003; received in revised form 11 July 2003; accepted 15 July 2003

Abstract

This study deals with the generation and characterization of various solid-state forms of celecoxib, a selective cyclooxygenase-2 (COX-2) inhibitor. The drug was subjected to polymorphic screen using different solvents to explore the possibility of existence of different solid forms. *N,N*-Dimethyl acetamide (DMA) and *N,N*-dimethyl formamide (DMF) yielded solvates in 1:1 stoichiometric ratio. Quench cooling of the melt resulted in amorphous form of the drug. All these solid-state forms were characterized by thermoanalytical (DSC, TGA, HSM), crystallographic (XRD), microscopic (polarized, SEM), spectroscopic (FTIR), and elemental analysis techniques. Solubility and van't Hoff studies were carried out for their thermodynamic interpretation. Influence of morphology of different solid-state forms on flow behavior was also investigated. Molecular modeling studies were used to elucidate the interaction between solute and solvent molecules in the solvate.

© 2003 Elsevier B.V. All rights reserved.

Keywords: Celecoxib; Polymorph; Pseudopolymorphs; Amorphous; Solid-state characterization

1. Introduction

Celecoxib, 4-[5-(4-methylphenyl)-3-(trifluoromethyl)-1*H*-pyrazol-1-yl] benzenesulphonamide (Fig. 1), belongs to a novel class of agents that selectively inhibit cyclooxygenase-2 (COX-2) enzymes. The introduction of this first selective COX-2 inhibitor (375-fold selectivity) (Clemett and Goa, 2000) in the pharmaceutical market revolutionized the treatment of osteoarthritis (OA), rheumatoid arthritis (RA), and management of pain. It is one of the top selling molecules (ranked 8th), with a worldwide sales of \$2614 million in year 2000 (Anonymous, 2001). US FDA has approved its use in OA, RA, and dysmenorrhea with dose strengths of 100–200 mg once/twice daily.

Celecoxib has a pK_a of 11.1, and its low aqueous solubility ($\cong 5 \mu\text{g/ml}$) contributes to high variability in absorption after oral administration (Paulson et al., 2001). Thus, it is important to enhance the solubility and dissolution rate of celecoxib to improve its overall oral bioavailability. Celecoxib exists as long needle-shaped crystals that impart

it some undesirable properties like cohesiveness, low bulk density and compressibility, which complicates its processing into solid dosage forms (Leonard and Patricia, 2001). These crystals result in poor blend uniformity, have a tendency to separate out, agglomerate and form a monolithic mass upon compression in the tablet die, making it difficult to process small quantities for formulation (Leonard and Patricia, 2001). Poor aqueous solubility and non-ideal physicochemical properties of celecoxib can be improved by utilizing alternate solid forms. A comparative assessment of physicochemical and physicochemical properties of various solid-state forms like, polymorphs, pseudopolymorphs, and amorphous form can help in selection of the best suited form. Alternate solid-state forms of paracetamol, phenobarbital, tolbutamide, etc. have been known to improve their tableting behavior (Brittain and Fiese, 1999). Amorphous forms of several drugs (cephalexin, indomethacin, iopanoic acid, frusemide, novobiocin, etc.) have shown enhanced dissolution rates and transient solubility, which translates into greater bioavailability (Jozwiakowski, 2000).

In the present study, various solid-state forms of celecoxib were generated and characterized by thermal, crystallographic, microscopic, spectroscopic, and elemental analysis techniques. These forms were also studied for aqueous

* Corresponding author. Tel.: +91-172-214682/214687; fax: +91-172-214692.

E-mail address: akbansal@niper.ac.in (A.K. Bansal).

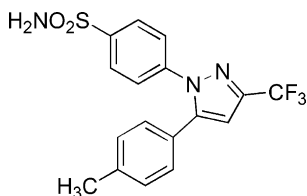


Fig. 1. Chemical structure of celecoxib.

solubility and van't Hoff plots were generated. Physicotechnical properties related to flow behaviour were also investigated. Molecular modeling of the solvates was carried out to explain the solute–solvent interactions in the crystal lattice.

2. Materials and methods

2.1. Materials

Celecoxib was gifted by Ranbaxy Research Laboratories, Gurgaon, India. All solvents were AR/HPLC grade.

2.2. Preparation of solid-state forms

Solvent recrystallization approach was used for polymorph screening. Solvents belonging to various classes as per ICH Q3C guidelines were used—acetone, ethanol, ethyl acetate, isopropanol, tetrahydrofuran (Class III); acetonitrile, chloroform, dichloromethane, *N,N*-dimethyl acetamide (DMA) and *N,N*-dimethyl formamide (DMF), methanol (Class II); and carbontetrachloride (Class I). Supersaturated solution of the drug was prepared by dissolving its excess amount in solvent at 60 °C, and the filtered solution was allowed to evaporate at room temperature. In case of high boiling solvents, like DMA and DMF, the solution was evaporated under reduced pressure, and kept overnight in refrigerator to allow crystallization. The crystals were collected and dried under reduced pressure at about 40 °C. The amorphous form was prepared by quench cooling where in the molten drug was spontaneously cooled over an ice bath.

2.3. Characterization

All characterization studies were performed in triplicate.

2.3.1. Differential scanning calorimetry (DSC)

DSC analysis was performed using Mettler Toledo 821^e DSC (Mettler Toledo, Switzerland) operating with Star^e software version Solaris 2.5.1. Temperature axis and cell constant were calibrated using indium. The samples were exposed to heating rates of 1, 5, and 10 °C/min over a temperature range of 25–200 °C under nitrogen purging (80 ml/min) in pin-holed aluminium pans.

2.3.2. Thermogravimetric analysis (TGA)

TGA was performed using Mettler Toledo 851^e TGA/SDTA in aluminium crucibles at a heating rate of 10 °C/min from 25 to 200 °C under nitrogen purging (20 ml/min).

2.3.3. Hot stage microscopy (HSM)

HSM was carried out using Leica DMLP polarized microscope and Leica LMV hot stage (Leica, Germany). Photographs were taken using RICOH XR-X 3000D camera (RICOH, Japan). Samples were mounted in air and/or silicone oil, and heated from 25 to 200 °C.

2.3.4. X-ray powder diffraction (XRD)

The XRD patterns of solid-state forms of celecoxib were measured with Philips PW 1729 X-ray diffractometer (Philips, Holland) using an online recorder (PM 8203A). Radiations generated from CuK α source and filtered through Ni filters with a wavelength of 0.154 nm at 20 mA and 35 kV were used to study the X-ray diffraction patterns. The instrument was operated over the 2θ range of 5–55°.

2.3.5. Fourier transform infrared spectroscopy (FTIR)

FTIR spectra of the samples were obtained on a Nicolet FTIR Impact 410 spectrophotometer (Nicolet, USA) equipped with OMNIC analyzing software, by the conventional KBr pellet method. Liquid samples were taken neat on KBr discs.

2.3.6. Scanning electron microscopy (SEM)

The samples were viewed under Jeol JSM 6100 scanning electron microscope (Jeol, Japan) after sputter coating with gold in Fine Coat Ion JFC 1100 sputter (Jeol, Japan).

2.3.7. Elemental analysis

Elemental analysis was carried out with an elemental analyzer (Elementar Vario El, Germany) instrument. About 5 mg of sample was taken in tin boat and analyzed using helium as the carrier gas at a flow rate of 200 ml/min. Combustion was carried out at 1150 °C and the reduction tube was maintained at 850 °C.

2.3.8. Solubility determination

Solubility was determined by placing an excess amount of sample in 5 ml of water (maintained at 37 °C) in screw-capped glass vials. Shaking at 200 rpm was achieved using shaker water bath (Heto, Denmark). Samples were withdrawn at regular intervals, filtered, and analyzed after appropriate dilution using UV spectrometer (Perkin-Elmer Lambda 20, USA) at a λ_{max} of 252 nm.

2.3.9. van't Hoff plot

Solubility of crystalline forms was determined in temperature range of 5–45 °C by placing an excess amount of sample in 30 ml of 50:50 methanol:water solution, maintained at specific temperature in jacketed glass bottles. The solution was stirred at 400 rpm on a magnetic stirrer. Samples were

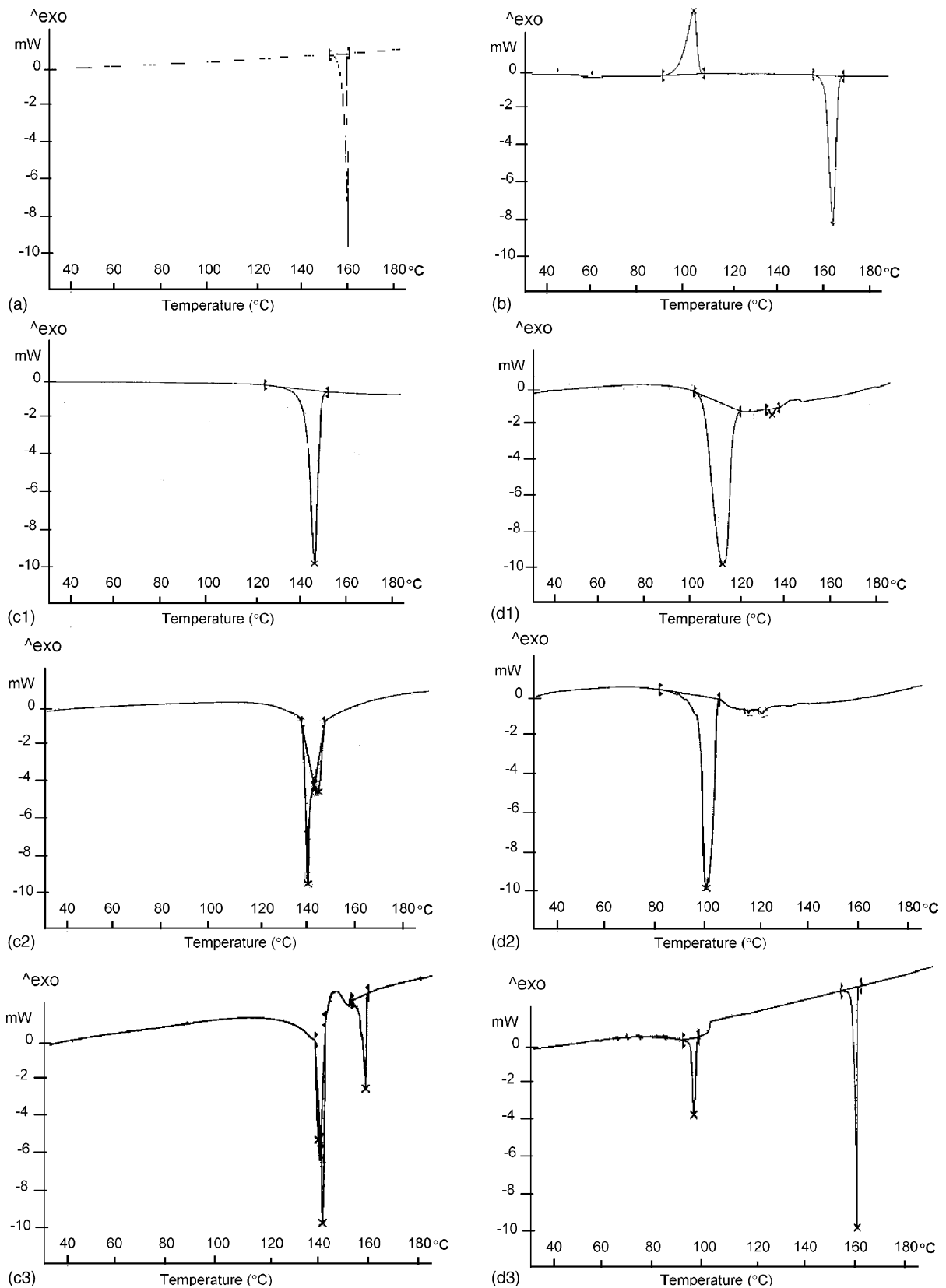


Fig. 2. DSC curves of various solid-state forms of celecoxib at different heating rates obtained using pin-holed aluminium pans: (a) celecoxib at a heating rate of 5 °C/min, (b) celecoxib-amorphous at a heating rate of 5 °C/min, (c1) CEL-DMA at a heating rate of 10 °C/min, (c2) CEL-DMA at a heating rate of 5 °C/min, (c3) CEL-DMA at a heating rate of 1 °C/min, (d1) CEL-DMF at a heating rate of 10 °C/min, (d2) CEL-DMF at a heating rate of 5 °C/min, (d3) CEL-DMF at a heating rate of 1 °C/min.

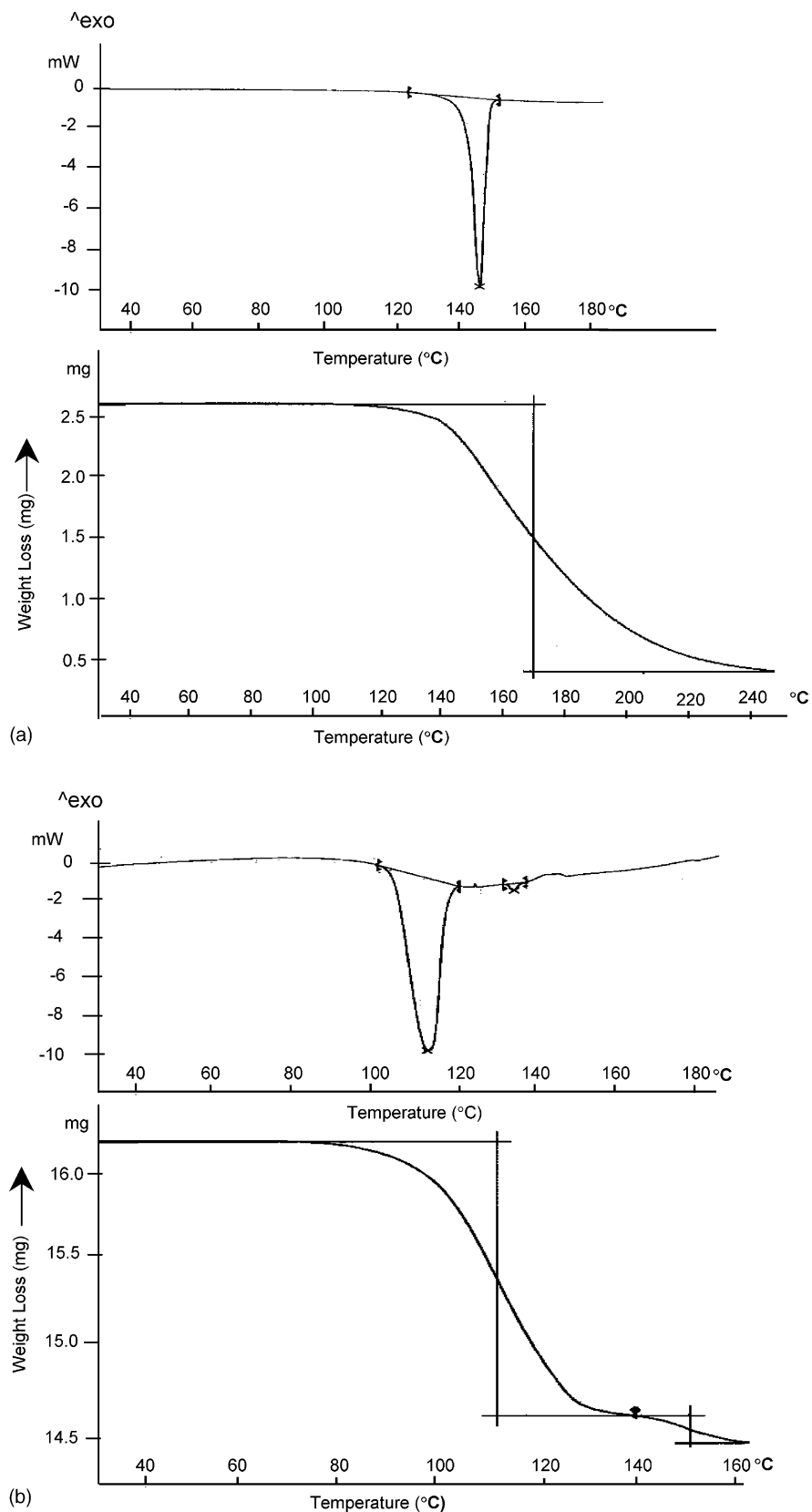


Fig. 3. TG curves of solvates of celecoxib along with DSC curves (at heating rate of 10°C/min). TG has been done in aluminium crucibles at heating rate of 10°C/min: (a) CEL-DMA, (b) CEL-DMF.

withdrawn at regular intervals and analyzed spectrophotometrically at 252 nm.

2.3.10. Measurement of flow properties

Bulk and tap density of samples was determined using Electrolab tap density tester (ETD-1020, India). Accurately weighed samples of known volume were tapped 300, 500, and 750 times, and change in volume was noted. The bulk density, tap density, Carr's index and Hausner ratio of different solid-state forms of celecoxib were calculated.

2.3.11. Molecular modeling

All calculations were performed using Sybyl 6.8 (Tripos Associates, Inc., 1699 S. Hanley, St. Louis, MI) installed on SGI octane2 system. The structure of celecoxib was obtained by few alterations of X-ray crystal structure co-ordinates of SC-558, extracted from 1CX2.pdb (Abola et al., 1987). The structures of solvent molecules, DMF and DMA, were built. Celecoxib molecule was solvated with DMF and DMA molecules using molecular silverware method. The charges were calculated using MMFF94 (Halgren, 1990). The solvated systems were then subjected to energy optimization using MMFF94 force field till the gradient convergence of 0.05 kcal/mol was reached.

2.3.12. Accelerated stability study

The various crystalline and amorphous products, packed in polyethylene laminated aluminium foils of thickness 0.04 mm, were stored under ICH specified accelerated stability conditions of storage for zones III and IV at 40 °C/75% RH. Crystalline samples, packed in screw-capped glass vials, were also subjected to accelerated stability study at these storage conditions in presence of light. The samples

were characterized using thermal and spectroscopic methods of analysis after 7, 15, 30, and 90 days.

3. Results and discussion

3.1. Solid-state screening: thermal methods

Crystalline celecoxib, quench cooled and solvent recrystallized products were initially characterized by DSC and TGA at heating rate of 10 °C/min for identification of any solid-state alterations. DSC analysis of celecoxib (Fig. 2a) showed a single endothermic event of fusion in the temperature range of 160.79–164.64 °C ($\Delta H_f = 90.07$ J/g). DSC analysis of solvent recrystallized products exhibited curves similar to crystalline celecoxib with identical values of melting points and heats of fusion, except for those obtained from DMF and DMA. Products recrystallized from DMF (hereafter mentioned as CEL-DMF) and DMA (hereafter mentioned as CEL-DMA) showed a shift of endothermic peak to lower temperature values and absence of peak in the above range, indicating the possibility of polymorph and/or pseudopolymorph formation.

These solvent recrystallized products were also characterized by TGA for assessing any solvate formation. Only CEL-DMF and CEL-DMA, exhibited weight loss of $16.082 \pm 0.4\%$ (molar ratio 1.008), and $18.904 \pm 0.5\%$ (molar ratio 1.012), respectively. When compared with DSC curves (Fig. 3), the TG curves of CEL-DMF and CEL-DMA confirmed the endothermic event observed in DSC to correspond to desolvation, hence indicating solvate formation with DMA and DMF. The experimentally determined percentage weight loss values were in close agreement with

Table 1

The enthalpy values corresponding to endothermic peaks obtained by DSC, at different heating rates, for different solid-state forms of celecoxib

Sample	Heating rate (°C/min)	Enthalpy ^a (kJ/mol)	Temperature ^b (°C) onset–peak–endset
Celecoxib	10	34.35 (90.07 J/g) ^c	160.79–161.80–164.64 ^e
	5	35.76 (93.77 J/g) ^c	161.42–162.55–164.36 ^e
	1	38.74 (101.59 J/g) ^c	162.87–163.50–164.11 ^e
CEL-DMA	10	8.57 (98.32 J/g) ^d	147.92–149.78–152.68 ^f
	5	4.11 (47.20 J/g) ^d	140.28–141.63–142.97 ^f
	1	2.90 (33.25 J/g) ^d	144.86–146.48–148.38 ^f
			140.63–141.47–142.26 ^f
		11.75 (30.82 J/g) ^c	142.45–142.91–144.57 ^f
			160.10–160.63–161.39 ^e
CEL-DMF	10	5.33 (61.19 J/g) ^d	99.71–102.10–106.77 ^f
	5	4.54 (62.05 J/g) ^d	99.80–101.92–106.69 ^f
	1	4.31 (58.90 J/g) ^d	98.89–101.72–103.97 ^f
			24.70 (64.77 J/g) ^c

^a Reported values are within ± 3 standard deviation.

^b Reported values are within ± 0.8 standard deviation.

^c Enthalpy of fusion.

^d Enthalpy of desolvation (sum of two desolvation peaks, in case of CEL-DMA).

^e Melting temperature.

^f Desolvation temperature.

theoretical values of 16.148 and 18.595% for CEL-DMF and CEL-DMA, respectively, representing a stoichiometry of nearly 1:1.

In order to trace the absence of melting endotherm in CEL-DMF and CEL-DMA at 10 °C/min, DSC analysis was performed at lower heating rates. Fig. 2c and d shows the DSC curves of CEL-DMA and CEL-DMF, respectively at different heating rates. A single endothermic peak was observed at heating rate of 5 °C/min for CEL-DMF, whereas additional endothermic events were observed at heating rate of 1 °C/min. The desolvation peak of CEL-DMA was observed to split into two at heating rate of 5 °C/min. This unresolved peak reflects the coupling of two simultaneous events. First, the breaking of interactions such as hydrogen bonds between DMA and celecoxib molecules, and second corresponding to desolvation, i.e. release of solvent molecules from the crystal lattice.

A complete desolvation and transition to high melting form was observed at a heating rate of 1 °C/min. CEL-DMA exhibited a recrystallization exothermic event after desolvation, followed by sharp endothermic peak at 161 °C/min corresponding to melting of crystalline form, into which it transforms after losing the solvent molecules. CEL-DMF also showed a sharp melting endotherm at 161 °C, characterizing the transformation of solvate to its crystalline counterpart. No significant change was observed in the desolvation enthalpies and temperature of CEL-DMF, with the change in heating rates. CEL-DMA, on the other hand, showed an increase in the enthalpy values with the increase in heating rate. The enthalpy and melting ranges of celecoxib, CEL-DMF and CEL-DMA are enlisted in Table 1. In addition, desolvation at higher temperature in CEL-DMA suggests relatively a stronger interactive force between DMA and celecoxib molecules and also greater compactness of crystal packing as compared to CEL-DMF.

Heating rates may greatly influence the kinetics and resolution of peaks in DSC curves (Giron, 1995). A high heating rate may not provide sufficient time for recrystallization, and only desolvation peak may be observed with the absence of melting peak of stable form. The shifting of location of the endothermic peak to higher temperature in CEL-DMA and the absence of exothermic peak at higher heating rates of 5 and 10 °C/min may be attributed to the time required for desolvation. The higher the heating rate, the lower is the time for desolvation to occur, which ultimately results in higher temperature for desolvation, and higher desolvation enthalpy (Behme et al., 1985). This is supported by the fact that at slowest heating rate of 1 °C/min, exothermic peak of recrystallization appeared suggesting desolvation and recrystallization to high melting form before melting.

DSC thermogram of amorphous form (Fig. 2b) showed glass transition onset peak at 50.84 ± 0.08 °C followed by recrystallization exotherm at 98.81 ± 0.1 °C ($\Delta H_C = 51.70 \pm 2$ J/g) and a melting endotherm at 164.40 ± 0.2 °C ($\Delta H_f = 84.86 \pm 4$ J/g). The glass transition and recrystal-

lization events observed in DSC prove the amorphous nature of quench cooled product (Kakumanu and Bansal, 2002). DSC can also be used to determine the degree of crystallinity, structural relaxation and crystallization kinetics of the amorphous form of celecoxib, as reported previously (Kakumanu and Bansal, 2002). The greatest advantages offered by the amorphous system in terms of higher solubility, improved bioavailability and performance characteristics can be attributed to its “excess properties” with respect to enthalpy, entropy, and free energy. The high degree of

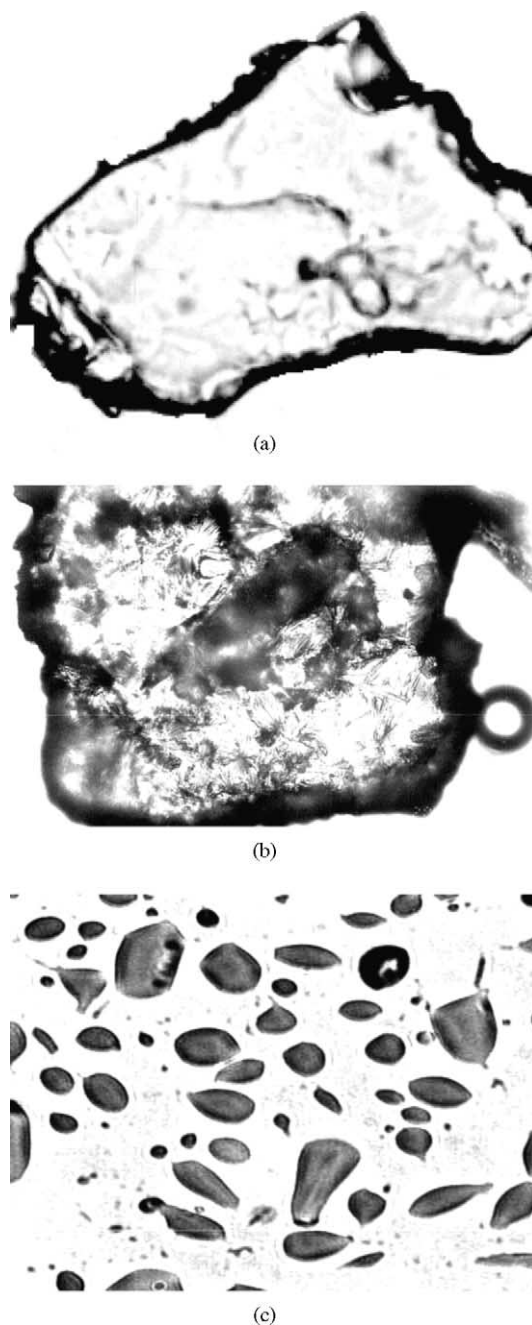


Fig. 4. HSM photographs of CEL-DMF mounted in silicone oil: (a) platy crystals at ambient temperature, (b) escape of solvent seen as bubbles between 104 and 106 °C, (c) droplets of melt at 161–164 °C.

molecular mobility in these high energy disordered systems leads to their spontaneous reversion to the thermodynamically stable crystalline form. Glass transition temperature, at which the molecular mobility is restricted, is a characteristic of amorphous systems and helps to distinguish between the amorphous and microcrystalline states (Yu, 2001).

Thermal events of solid-state forms of celecoxib were also determined with HSM, and were found to be in close agreement with those obtained from DSC and TGA. When observed in the presence of silicone oil, loss of solvent was viewed as the generation of bubbles (between 140–146 °C in CEL-DMA and 98–106 °C in CEL-DMF) from within the

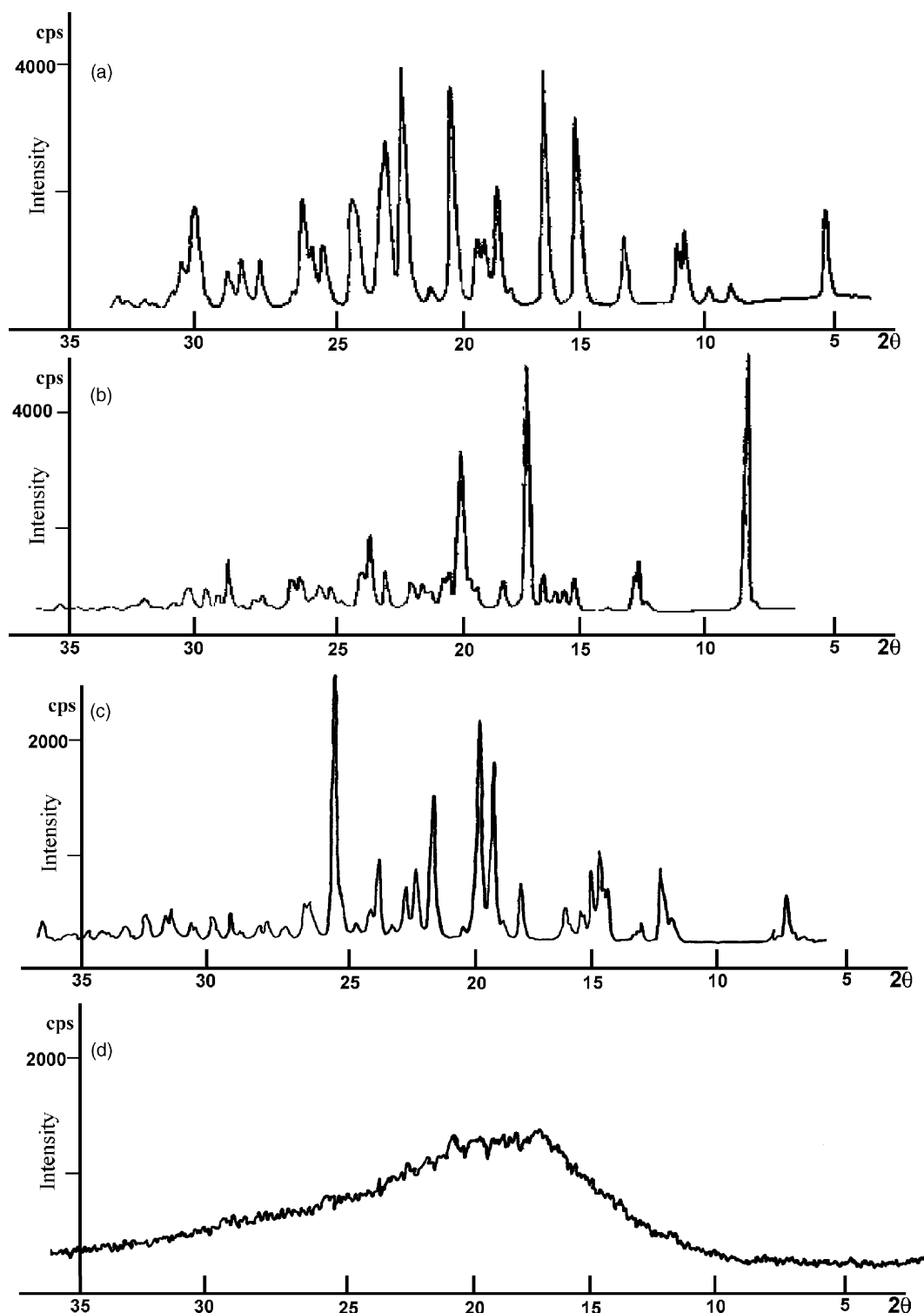


Fig. 5. X-ray diffractograms of various solid-state forms of celecoxib: (a) celecoxib, (b) CEL-DMA, (c) CEL-DMF, (d) CEL-amorphous.

crystal lattice (Fig. 4). Desolvation upon heating involves initial molecular loosening at the solvent sites and rupture of plate habit of celecoxib solvates to provide diffusion paths for escape of solvent molecules, and complete reorganization to needle habit of celecoxib which melt near 161 °C, as observed in DSC endotherms. In the amorphous form, recrystallization was seen as origination of needles at around 85–90 °C, followed by melting at around 165–168 °C. The amorphous product being a high energy disordered form, experiences a significant enhancement in molecular mobility above glass transition temperature leading to loss of energy in terms of an exothermic event corresponding to molecular rearrangement to low energy ordered crystalline form (Hancock and Zografi, 1997).

3.2. XRD

XRD is one of the most sensitive and a foolproof method for solid-state characterization as the results are obtained directly from the molecular arrangements of the crystalline material (Chao and Vail, 1987). Fig. 5 shows the XRD patterns of solid-state forms of celecoxib. Crystalline forms of celecoxib showed sharp diffraction peaks. The crystal lattice parameters of celecoxib have been reported as: $a = 10.136$, $b = 16.778$, $c = 5.066$, $\alpha = 97.62$, $\beta = 100.65$, and $\gamma = 95.95$, with triclinic unit cells (Dev et al., 1999). XRD pat-

tern of each solvate was featured by a scattering peak unique to each form at a scattering angle (2θ) where no diffraction was observed for the other form hence, permitting an unambiguous identification and distinction between them. The distinct differences in the diffraction patterns of celecoxib, CEL-DMA and CEL-DMF are attributed to modifications in the arrangement of molecules in the crystal lattice. On the other hand, the XRD pattern of amorphous form was devoid of diffraction peaks and a halo pattern was observed, confirming the lack of three-dimensional long range ordered structure.

3.3. Microscopy

Crystal morphology plays a valuable role in pharmaceutical processing and product development of solid dosage forms. Differences in crystal habit may strongly influence the particle orientation, modify flowability, packing, compaction, compressibility and dissolution characteristics of a drug powder. Solid–liquid interface interactions can alter the roundness of the interfaces, change crystal growth kinetics and enhance or inhibit growth at certain crystal faces, resulting in different habits (acicular, plates, tabular, bladed, prismatic, etc.) (Tiwary, 2001).

The morphological features of various solid-state forms of celecoxib were visually examined using light microscopy.

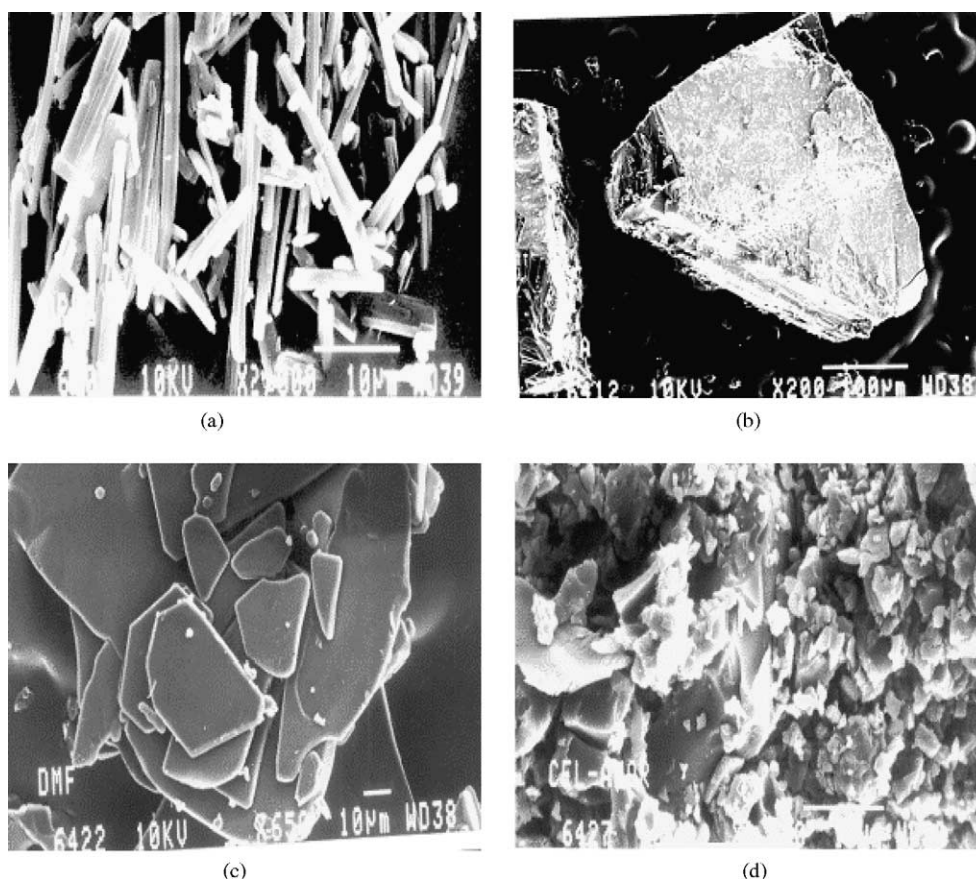


Fig. 6. SEM photographs of various solid-state forms of CEL: (a) CEL, (b) CEL-DMA, (c) CEL-DMF, (d) celecoxib-amorphous.

The stable crystalline form of celecoxib occurs as fine needles. On the other hand, both the solvate forms were found to exhibit plate-like crystal habit. The irregularity in morphology substantiates the amorphous nature of the quench cooled product.

SEM photographs (Fig. 6) showed a distinct difference in the morphology of different solid-states forms. Celecoxib consisted of blunt-ended needle-shaped crystals. Plates of CEL-DMF had smooth surface in contrast to the rough surfaced CEL-DMA platy crystals. Amorphous form appeared as aggregates of irregularly shaped particles.

Celecoxib crystals were found to exist in polycrystalline form with parallel grain boundaries when observed under cross polarizers. The polycrystalline behavior was characterized by the appearance of multi-colored (green, blue, pink, and yellow) grains arranged in parallel fashion. The solvates also retained the polycrystalline nature but with irregularly arranged grains. Triclinic crystals of celecoxib and solvates exhibit optical anisotropy as they displayed numerous optical effects, produced birefringes and showed regular extinction of plane polarized light on each 90° rotation of microscope stage. On the contrary, absence of birefringes under polarized light showed the amorphous behavior of quench cooled product.

3.4. FTIR spectroscopy

FTIR spectroscopy has been successfully used for exploring the differences in molecular conformations, crystal

packing and hydrogen bonding arrangements for different solid-state forms of an organic compound (Brittain, 1997). Spectral variations originate due to alteration in bonds that exhibit characteristic vibrational frequencies, leading to frequency shifts and splitting in absorption peaks. The FTIR spectra of celecoxib (Fig. 7a) showed a characteristic S=O symmetric and asymmetric stretching at 1164 and 1347 cm^{-1} , respectively. Medium intensity bands at 3338 and 3232 cm^{-1} were seen as a doublet, which are attributed to the N–H stretching vibration of $-\text{SO}_2\text{NH}_2$ group.

The C–N stretching band observed at 1397 and 1388 cm^{-1} for DMA and DMF (Fig. 7b and c'), respectively shifted to lower frequencies of 1374 and 1379 cm^{-1} in CEL-DMA and CEL-DMF (Fig. 7b' and c), respectively. Lowering of frequencies was also seen for C=O stretching bands from 1635 to 1613 cm^{-1} in CEL-DMA (Fig. 7b'), and from 1673 to 1651 cm^{-1} in CEL-DMF (Fig. 7c), as compared to neat solvents. These shifts in frequencies indicate the possibility of hydrogen bonding between the $-\text{C}=\text{O}$ group of solvents and $-\text{NH}_2$ group of sulfonamide moiety present in celecoxib. This hydrogen bonding leads to increase in negative charge over oxygen atom caused by shift of π electrons of $-\text{C}=\text{O}$ group, resulting in the weakening of its double bond character (shown in Scheme 1). Hydrogen bonding alters the force constant of C=O as well as C–N, thus altering the frequency of stretching and bending vibrations.

The bands corresponding to N–H stretching of $-\text{NH}_2$ group became diffused and broadened in case of amorphous form as shown in Fig. 7d, and also a shift to lower frequency

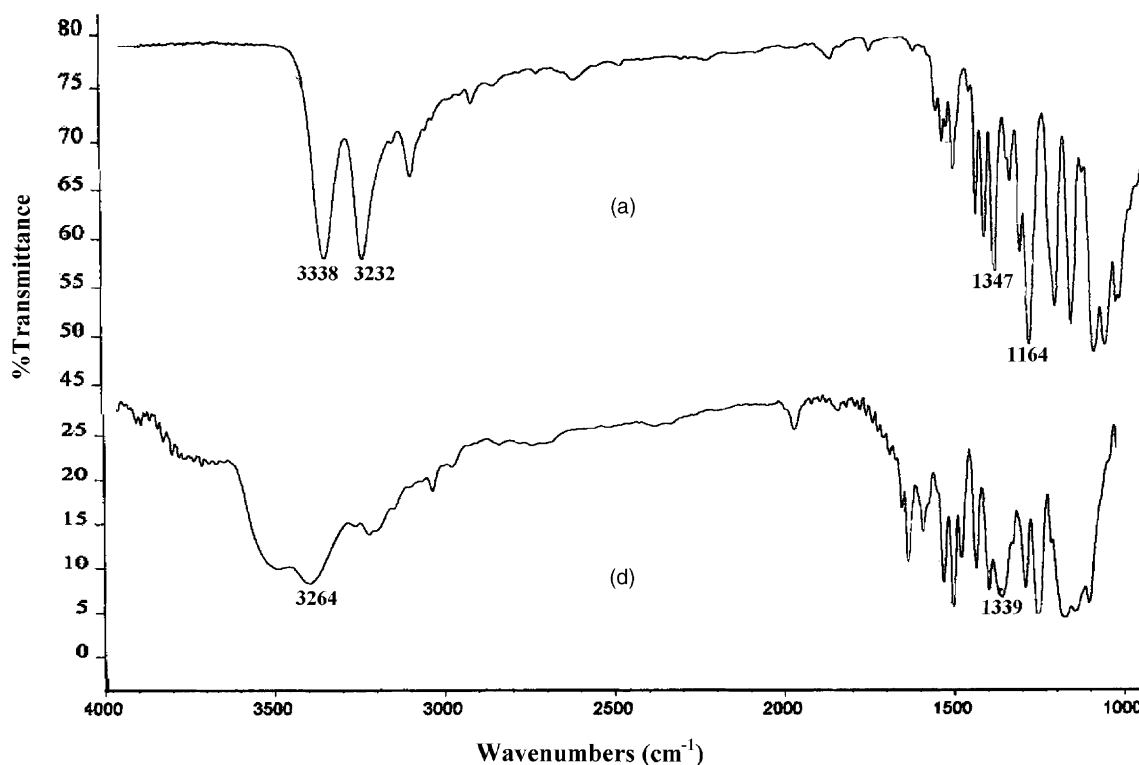


Fig. 7. IR spectra: (a) celecoxib, (b) DMA, (b') CEL-DMA, (c) CEL-DMF, (c') DMF, (d) celecoxib-amorphous.

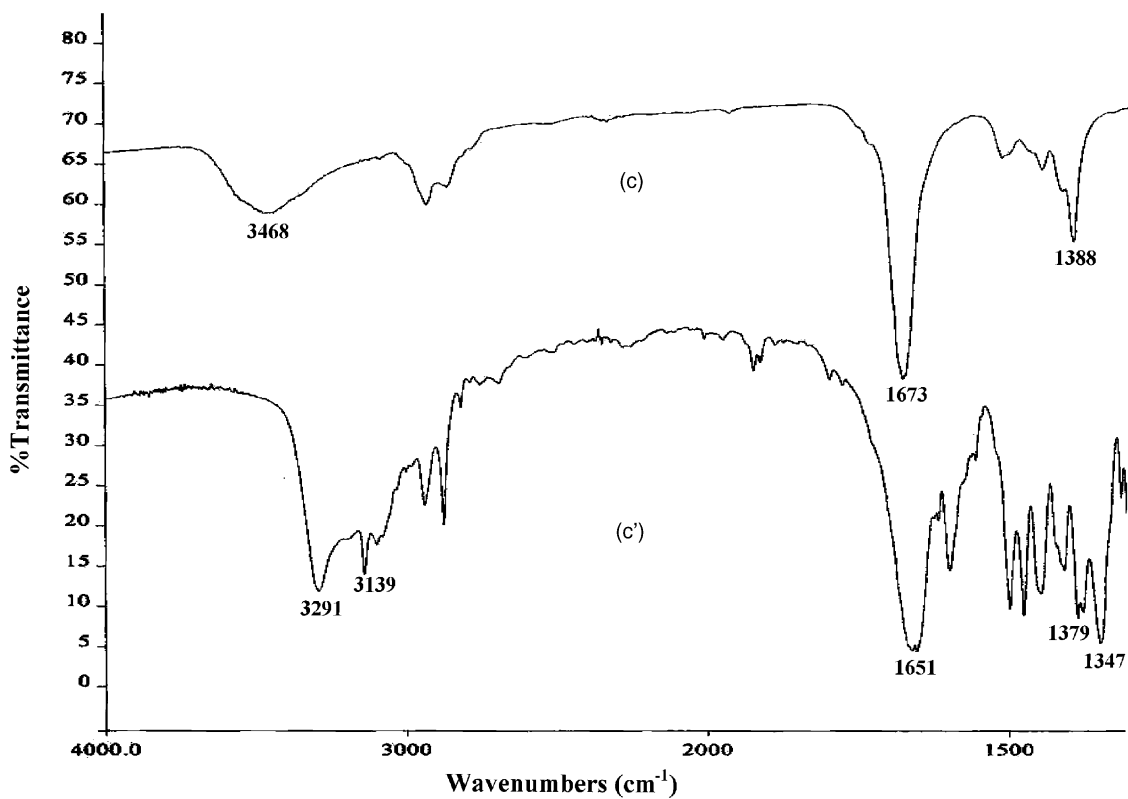
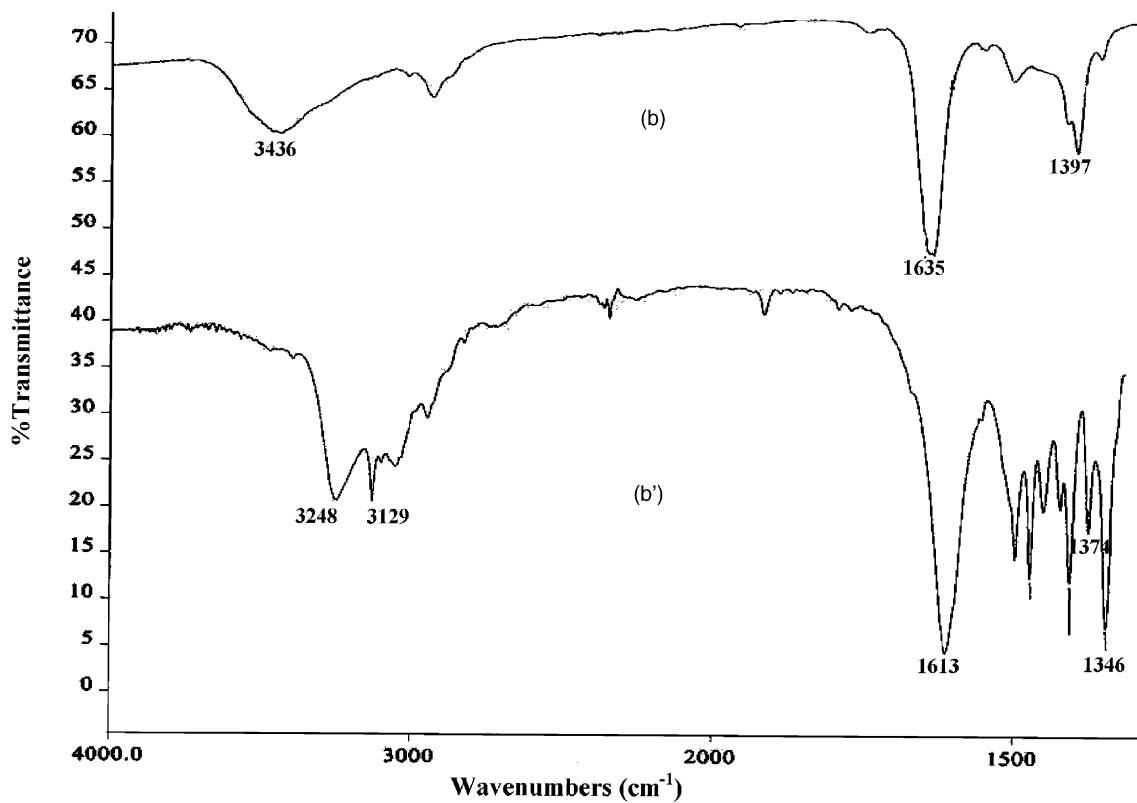
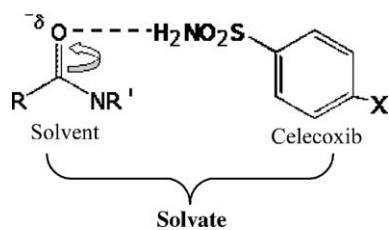


Fig. 7. (Continued).



Scheme 1.

(1339 cm^{-1}) was observed in asymmetric stretching of $-\text{SO}_2$ group. This clearly indicates the participation of $-\text{NH}_2$ and $-\text{SO}_2$ groups in intermolecular hydrogen bonding between celecoxib molecules. The spatial arrangement of celecoxib molecules in crystal lattice does not allow intermolecular hydrogen bonding which starts to occur once the orderliness of crystalline lattice is disturbed by formation of amorphous form.

3.5. Elemental analysis

Results of elemental analysis are summarized in Table 2. These results agreed with the theoretical values for 1:1 stoichiometry as evidenced by TGA results and the molar ratios.

3.6. Solubility determination

Solubility determination is of vital importance for pharmaceutical compounds, especially BCS Class II drugs. CEL-DMA, CEL-DMF, and amorphous form gave higher peak solubility values of $4.98 \pm 0.4 \mu\text{g/ml}$, $3.62 \pm 0.1 \mu\text{g/ml}$, and $4.66 \pm 0.6 \mu\text{g/ml}$, respectively, as compared to $3.56 \pm 0.2 \mu\text{g/ml}$ for higher melting crystalline form. Inclusion of organic solvents in the solvated form tends to increase solubility and dissolution rate, presumably by weakening the crystalline lattice (Brittain and Grant, 1999). The amorphous form being the high energy state, due to lack of long range order, produces a greater molecular mobility and thermodynamic escaping tendency leading to faster dissolution rates and higher solubility (Hancock and Zografi, 1997).

The solvated and amorphous forms attained peak concentrations within 15 min, but the initial solubility advantage was lost and solubility values similar to the crystalline form were reached within 1 h for all the systems. This is a result of solvent-mediated transformation of solvates and amorphous form to the less soluble crystalline form. This

Table 2
Percentage composition of different elements present in various solid-state forms of celecoxib

Sample	% Carbon	% Nitrogen	% Hydrogen	% Sulphur
Celecoxib	53.61 (53.49) ^a	11.34 (11.01) ^a	3.89 (3.67) ^a	8.72 (8.39) ^a
CEL-DMA	53.83 (53.78) ^a	12.02 (11.95) ^a	4.93 (4.91) ^a	6.91 (6.83) ^a
CEL-DMF	52.39 (52.80) ^a	12.30 (12.30) ^a	4.81 (4.62) ^a	6.97 (7.04) ^a

^a Theoretical values for 1:1 stoichiometry are given in parenthesis.

phenomenon was also visually observed under the microscope, as formation of needle-shaped crystals in presence of water. Such solution-mediated phase transformations depend upon the solution phase to provide the mobility necessary to help molecules rearrange to the most stable form. After peak solubility is achieved, the system reaches a pseudoequilibrium state prior to conversion to the stable form. This rearrangement is caused due to the crystallization of stable solid, from its supersaturated solution, formed due to dissolution of metastable form.

3.7. van't Hoff plot

Plots of logarithmic values of peak concentration versus inverse of temperature resulted in superimposable curves of celecoxib and its solvates (Fig. 8). This is due to the transformation of solvates back to the high melting needle-shaped crystals in the presence of solvent. Hence, for such systems, where the solvates revert back to the stable form in the presence of a solvent, equilibrium solubility and van't Hoff plots cannot be used for their characterization.

3.8. Flow properties

The bulk density, tap density, Carr's index, and Hausner ratio of various solid-state forms of celecoxib are enlisted

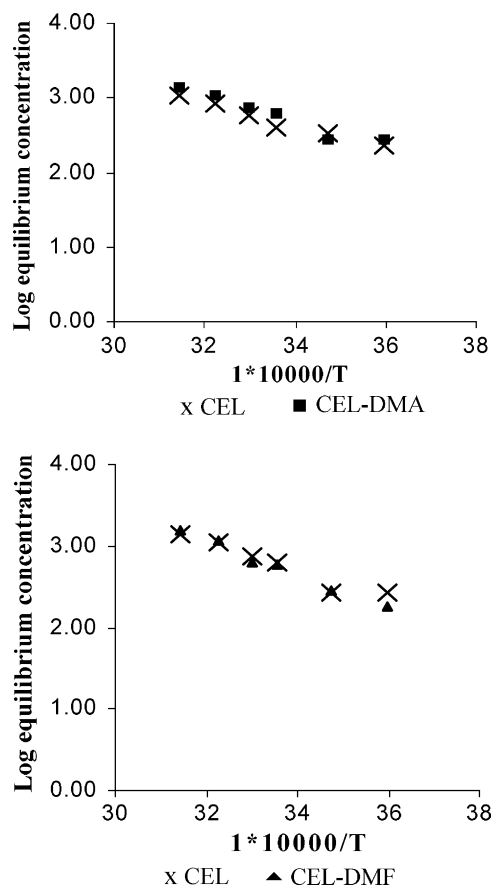


Fig. 8. van't Hoff plots of celecoxib and its solvates.

Table 3
Density and other flow parameters of different solid-state forms of celecoxib

Sample	Bulk density (g/ml)	Tap density (g/ml)	Carr's index (%)	Hausner ratio
Celecoxib	0.362 ± 0.04	0.517 ± 0.01	29.961 ± 1	1.428 ± 0.1
CEL-DMA	0.564 ± 0.03	0.729 ± 0.03	22.542 ± 1	1.291 ± 0.1
CEL-DMF	0.445 ± 0.04	0.645 ± 0.02	31.049 ± 1	1.450 ± 0.1
Celecoxib-amorphous	0.475 ± 0.02	0.698 ± 0.02	31.964 ± 2	1.470 ± 0.1

in Table 3. The stable form existing as cohesive needles showed the poorest flow properties, though not much differences were seen in the flowability of other forms. CEL-DMA showed the best flowability which can further be enhanced by the addition of glidant.

3.9. Molecular modeling

Molecular modeling studies confirmed the hydrogen bonding between sulphonyl amino group of celecoxib and carbonyl group of solvents (Fig. 9a and b), as observed by the shift in FTIR vibrational peaks of CEL-DMA and CEL-DMF. The solvation energies were found to be -24.668 and -27.823 kcal/mol for CEL-DMA and CEL-DMF, respectively. The hydrogen bonding observed in solvated systems are: CEL-DMF: N–H...O 2.693 Å, H...O 1.679 Å and CEL-DMA: N–H...O 2.725 Å, H...O 1.723 Å.

3.10. Accelerated stability study

Crystalline samples stored at 40 °C/75% RH showed no change in morphology, desolvation, and melting behaviors,

when viewed under hot stage microscope. CEL-DMA and CEL-DMF lost solvent molecules at about 141–148 °C and 98–100 °C, respectively, and transformed back to needle-shaped crystals that melt near 160–162 °C, as in case of freshly prepared samples. Thermal analysis of CEL-DMA and CEL-DMF samples stored for 3 months showed desolvation endotherms at 147.73 ± 0.5 °C ($\Delta H_D = 68.83 \pm 3$ J/g) and 102.6 ± 0.3 °C ($\Delta H_D = 61.61 \pm 4$ J/g), respectively. Also, samples were found to be stable under accelerated stability conditions of storage in presence of light.

The transition behavior of amorphous form was also investigated since, it is a metastable state and might crystallize during storage. The amorphous sample was found to revert back to the crystalline form within 7 days of storage under accelerated stability conditions. This transformation was viewed as the absence of glass transition and crystallization exotherm (characteristic for amorphous systems) from DSC, and appearance of only a sharp endothermic peak ($\Delta H_C = 92.09 \pm 2$ J/g) which corresponded to the melting of crystalline form. FTIR spectra of these samples also showed the reappearance of N–H stretching doublet at 3236 and 3346 cm^{-1} unique to the crystalline form.

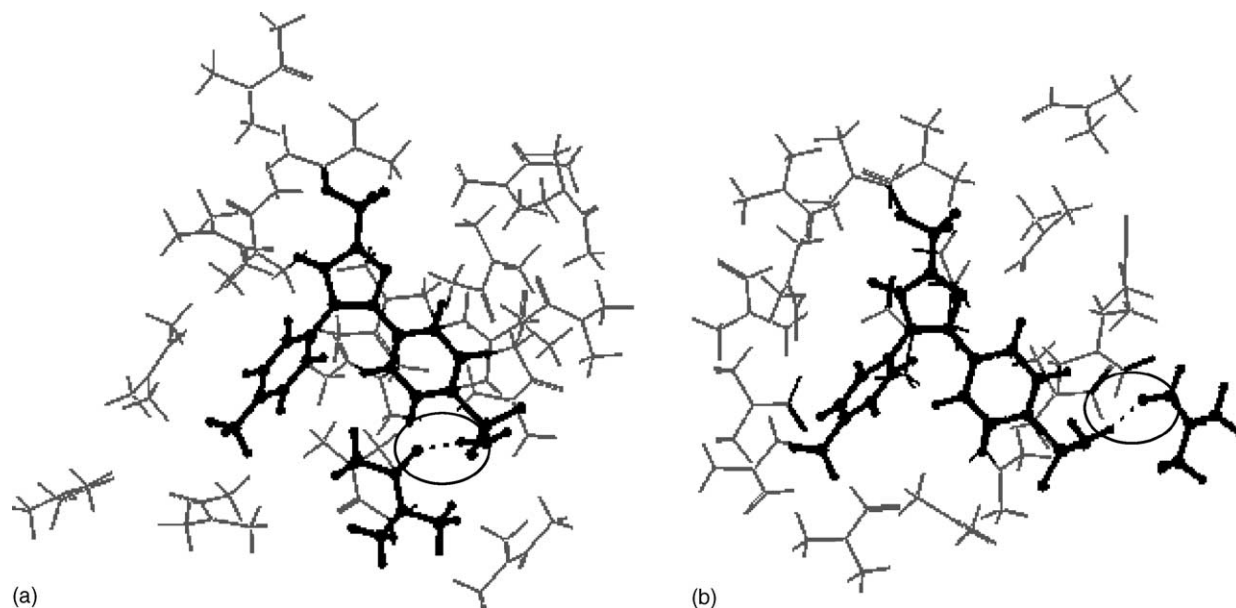


Fig. 9. Stereoview of celecoxib solvates: (a) CEL-DMA solvated model, (b) CEL-DMF solvated model. Celecoxib and solvent molecule in the solvate is represented by ball and stick model. The dotted line (encircled) represents the hydrogen bonding between the carbonyl group of solvent and amino group of sulfonamide moiety of celecoxib.

4. Conclusion

Celecoxib was found to form solvates with DMA and DMF in 1:1 stoichiometric ratio. Quench cooling of the melt resulted in the generation of amorphous form. The solvates exhibited plate-like crystal habit in contrast to needle-like crystal habit of the stable form, with polycrystalline behavior. The X-ray diffractograms and FTIR absorption spectra of the crystalline and amorphous forms also differed distinctively. The absence of peaks in X-ray diffractograms and the irregular morphology of the quench cooled product inferred its disorderliness. The desolvation peak in DSC curves, weight loss in TGA and generation of bubbles in HSM further confirmed the existence of solvent in the crystal lattice. Elemental analysis and molecular modeling studies confirmed the molar ratio and the bond formation of solvent molecules with the drug. Recrystallization of the amorphous form was observed in DSC and HSM. The higher aqueous solubility of solvates and amorphous forms indicate the usefulness of solid-state manipulation as a tool to overcome biopharmaceutical hurdles in drug delivery. The solubility benefits from the amorphous form can be exploited if it can be “stabilized” against reversion to stable crystalline form. Further, the thermodynamics of these solid-state forms can provide a greater insight into their physical stability and feasibility for formulation development.

Acknowledgements

The authors thank Ranbaxy Research Laboratories, Gurgaon, India, for providing the celecoxib sample. Services provided by Central Instrumentation Laboratory, NIPER, India, and Regional Sophisticated Instrumentation Centre, Punjab University, India are gratefully acknowledged.

References

- Abola, E.E., Berstein, F.C., Bryant, S.H., Koetzle, T.F., Weng, J., 1987. Protein data bank, crystallographic databases—information content, software systems, scientific applications. In: Allen, F.H., Berjerhoff, G., Sievers, R. (Eds.), Data Commission of the International Union of Crystallography. Bonn, pp. 171–200.
- Anonymous, 2001. 50 top selling drugs ranked by worldwide sales for 2000, Patent scan—a monthly proactive patents bulletin for pharmaceutical industry. *Med. Ad News* 2 (12).
- Behme, R.J., Brooke, D., Farney, R.F., Kensler, T.T., 1985. Characterization of polymorphism of gepirone hydrochloride. *J. Pharm. Sci.* 74, 1041–1046.
- Brittain, H., 1997. Spectral methods for the characterization of polymorphs and solvates. *J. Pharm. Sci.* 86, 405–412.
- Brittain, H., Fiese, E., 1999. Effects of pharmaceutical processing on drug polymorphs and solvates. In: Swarbrick, J. (Ed.), *Polymorphism in Pharmaceutical Solids*. Marcel Dekker, New York, pp. 331–365.
- Brittain, H.G., Grant, D.J.W., 1999. Effects of polymorphism and solid-state solvation on solubility and dissolution rate. In: Swarbrick, J. (Ed.), *Polymorphism in Pharmaceutical Solids*. Marcel Dekker, New York, pp. 279–330.
- Chao, R.S., Vail, K.C., 1987. Polymorphism of 1,2-dihydro-6-neopentyl-2-oxonicotinic acid: characterization, interconversion, and quantitation. *Pharm. Res.* 4, 429–432.
- Clemett, D., Goa, K.L., 2000. Celecoxib a review of its use in osteoarthritis, rheumatoid arthritis and acute pain. *Drugs* 59, 957–980.
- Dev, R.V., Rekha, K.S., Vyas, K., Mohanti, S.B., Kumar, P.R., Reddy, G.O., 1999. Celecoxib, a COX-II inhibitor. *Acta Cryst.* C55.
- Giron, D., 1995. Thermal analysis and calorimetric methods in the characterization of polymorphs and solvates. *Thermochim. Acta* 248, 1–59.
- Halgren, T., 1990. MOME force field parameters. *J. Am. Chem. Soc.* 112, 4710–4725.
- Hancock, B., Zografi, G., 1997. Characterization and significance of the amorphous state in pharmaceutical systems. *J. Pharm. Sci.* 86, 1–12.
- Jozwiakowski, M., 2000. Alteration of the solid state of the drug substance: polymorphs, solvates, and amorphous forms. In: Liu, R. (Ed.), *Water Insoluble Drug Formulation*. Interpharm Press, Colorado, pp. 525–562.
- Kakumanu, V., Bansal, A., 2002. Enthalpy relaxation studies of celecoxib amorphous mixtures. *Pharm. Res.* 19, 1873–1878.
- Leonard, F., Patricia, M., 2001. Polymorphic crystalline forms of celecoxib. WO 01/42222 A1.
- Paulson, S., Vaughn, M., Jessen, S., Lawal, Y., Gresk, C., Yan, B., Maziasz, T., Cook, C., Karim, A., 2001. Pharmacokinetics of celecoxib after oral administration in dogs and humans: effect of food and site of absorption. *J. Pharmacol. Exp. Ther.* 297, 638–645.
- Tiwary, A.K., 2001. Modification of crystal habit and its role in dosage form performance. *Drug Dev. Ind. Pharm.* 27, 699–709.
- Yu, L., 2001. Amorphous pharmaceutical solids: preparation, characterization and stabilization. *Adv. Drug Del. Rev.* 48, 27–42.